Results in Physics 7 (2017) 3203–3208

Contents lists available at ScienceDirect

Results in Physics

journal homepage: www.journals.elsevier.com/results-in-physics

Structural, morphological and magnetic properties of Eu-doped $CoFe_2O_4$ nano-ferrites

Aiman Zubair [a], Zahoor Ahmad [b], Azhar Mahmood [c], Weng-Chon Cheong [c], Irshad Ali [d], Muhammad Azhar Khan [e,*], Adeel Hussain Chughtai [a], Muhammad Naeem Ashiq [a,*]

[a] Institute of Chemical Sciences, Bahauddin Zakariya University, Multan 60800, Pakistan
[b] Department of Chemistry, University of Engineering and Technology (UET), Lahore, Pakistan
[c] Department of Chemistry, Tsinghua University, Beijing 100084, China
[d] Department of Physics, Bahauddin Zakariya University, Multan 60800, Pakistan
[e] Department of Physics, The Islamia University of Bahawalpur, Bahawalpur 63100, Pakistan

ARTICLE INFO

Article history:
Received 27 March 2017
Received in revised form 15 August 2017
Accepted 19 August 2017
Available online 24 August 2017

Keywords:
Europium doped cobalt ferrites
Co-precipitation
X-ray diffraction
Scanning electron microscopy
Magnetic properties

ABSTRACT

Europium (Eu) doped spinel cobalt ferrites having composition $CoEu_xFe_{2-x}O_4$ where x = 0.00, 0.03, 0.06, 0.09, 0.12 were fabricated by co-precipitation route. In order to observe the phase development of the ferrite samples, thermo-gravimetric analysis was carried out. The synthesized samples were subjected to X-ray diffraction analysis for structural investigation. All the samples were found to constitute face centered cubic (FCC) spinel structure belonging to Fd3m space group. Scanning electron microscopy revealed the formation of nanocrystalline grains with spherical shape. Energy dispersive X-ray spectra confirmed the presence of Co, Eu, Fe and O elements with no existence of any impurity. The magnetic hysteresis curves measured at room temperature exhibited ferrimagnetic behavior with maximum saturation magnetization (Ms) of 65 emu/g and coercivity (Hc) of 966 Oe. The origin of ferrimagnetism in Eu doped cobalt ferrites was discussed in detail with reverence to the allocation of Co^{2+} and Fe^{3+} ions within the spinel lattice. The overall coercivity was increased (944–966 Oe) and magnetization was decreased (65–46 emu/g) with the substitution of Eu^{3+}. The enhancement of former is ascribed to the transition from multi domain to single domain state and reduction in lateral is attributed to the incorporation of nonmagnetic Eu ions for Fe, resulting in weak superexchange interactions.

Introduction

Ferrites have become the subject of several explorations for many years not only due to their scientific and technological applications in the fields of electronics, magneto-electronics optoelectronics but also in the field of electrochemical science and technology, magnetic fluids, high frequency data storage and biotechnology [1,2]. In recent times, ferrite compounds have also attained great consideration for their potential use as electrode materials in solid oxide fuel cells and Li-ion batteries [3–5]. These materials show notable properties such as large permeability at high frequency, large saturation magnetization and high dc electrical resistivity, which are striking for use in magneto-electronics and electronics fields. Cobalt ferrite (CFO), being the most adaptable hard ferrimagnetic material, reveals exclusive characteristics such as high Curie temperature T_c (~520 °C), high magnetocrystalline anisotropy, high coercivity value (~5300 Oe), reasonable saturation magnetization (~70 emu/g) at room temperature, large magneto-optic Kerr effect and Faraday rotation [6–8]. In addition, cobalt ferrite play a vital role in lithium batteries as cathode material as well as in super capacitors [9]. However, structural, spectral, electrical, optical, dielectric and magnetic properties of CFO are very responsive to the method of preparation, surface morphology and size of the particles, reactive/processing atmosphere and cation addition in the crystal structure of host material that substitute for Fe^{2+}/Fe^{3+} ions [9,10]. The impact of the rare earth (RE) ion substitution on the magnetic properties of the ferrite materials have been studied by many researchers, particularly for using them in applications such as magneto-optical (MO) recording, magneto-optical sensors and hyperthermia treatment [11–13]. The incorporation of RE ions for Co and Fe ferrite causes the lattice strain and structural disorder which allows to tune the electrical and dielectric properties [14,15]. The objective of present work is to know the Eu-doping induced effects on the physical, structural,

* Corresponding authors.
E-mail addresses: azhar.khan@iub.edu.pk (M.A. Khan), naeemashiqqau@yahoo.com (M.N. Ashiq).

http://dx.doi.org/10.1016/j.rinp.2017.08.035
2211-3797/

morphological and magnetic properties of cobalt ferrite. It is well renowned that RE ions possess unpaired 4 f electrons as well as the strong spin-orbit coupling, thus addition of RE ions into spinel ferrite lattice, leads to the occurrence of 3 d–4 f coupling, which can vary the structural, electrical, spectral and magnetic properties of spinel ferrites. Hence the substitution of RE ions is becoming a capable way of enhancing the structural and electromagnetic properties [16]. The overall electromagnetic properties of ferrite materials depend upon ions nature, ionic sizes, their oxidation states and also their distribution among the tetrahedral (A) and octahedral (B) sites [14]. Eu^{3+} is considered to be non-magnetic at the room temperature. However, in CFO lattice, the substitution of Eu^{3+} for Fe^{3+} provokes significant saturation magnetization, which is enormously valuable to tailor the performance and properties of cobalt ferrites [17]. Additionally, in association with the variation of f-shell electron orbital contribution to the magnetic interactions, Eu^{3+} can be either anisotropic or isotropic. Therefore, by introducing the trivalent rare earth Eu^{3+} cations into the inverse spinel lattice will also provoke the Fe^{3+}–RE^{3+} interactions, which could change the subsequent magnetic properties [18–20]. Here in order to enhance the structural, morphological and magnetic behavior of cobalt ferrite, we have systematically incorporated Eu^{3+} ions and fabricated the materials by co-precipitation method. TGA, XRD, SEM, EDX and magnetization measurements were taken to understand our inspection of structural and magnetic behavior in Eu substituted cobalt ferrite.

Materials and method

Eu doped CFO were synthesized by using the following materials: cobalt nitrate $Co(NO_3)_2{\cdot}6H_2O$ (Sigma Aldrich 99.999%), ferric nitrate $Fe(NO_3)_3{\cdot}9H_2O$ (Sigma Aldrich 98.0%), europium nitrate $Eu(NO_3)_3{\cdot}5H_2O$ (Sigma Aldrich 99.9%) and ammonia solution. Cobalt ferrite (CFO) and europium substituted cobalt ferrite (CEuFO) nanoparticles were synthesized following co-precipitation method. The details of synthesis process is as follows: stoichiometric amounts of $Fe(NO_3)_3{\cdot}9H_2O$, $Co(NO_3)_2{\cdot}6H_2O$ and $Eu(NO_3)_3{\cdot}5H_2O$ were weighed and then dissolved in distilled water and stirred for 10–15 min. The aqueous ammonia (2 M) was added to the mixture of the prepared solution to keep up the pH value 10. After attaining required pH, the solution was subjected to constant uniform stirring for 5 h. After that, the precipitated material was filtered and washed several times with distilled water and then dried at 80 °C for 3 h. The un-annealed powder (CFO) was characterized for thermal decomposition processes by thermo-gravimetric analysis (TGA/DTA) instrument model; Mettler Toledo GC 200) under heating rate of 10 °C/min. The obtained final powder was treated for annealing at 800 °C for 8 h. X-ray diffraction statistics were collected using Bruker D8-ADVANDED X-ray diffractometer with Cu-Kα radiation (λ = 1.54178 Å). High-field (±3 T) magnetization measurements were performed at room temperature with the help of a quantum design vibrating sample magnetometer (VSM: Model 6000).

Results and discussion

Thermal analysis

Thermo-gravimetric analysis (TGA) along with the differential thermal analysis (DTA) of as prepared sample was carried out to differentiate the thermal decomposition till the formation of ferrite [13]. Fig. 1 exhibits the TGA and DTA curves attained from the sample with chemical composition $CoFe_2O_4$ ferrite. The thermal behavior of investigated sample helps to examine the annealing temperature necessary for the ferrite formation. In TGA curve,

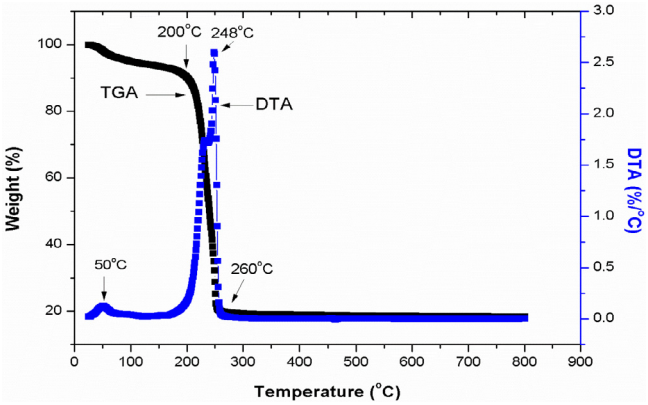

Fig. 1. TGA/DTA curves of $CoFe_2O_4$ ferrite nanoparticles.

the weight loss at temperature 200 °C is 10% and it drops to 79% at 260.5 °C. These weight losses occur due to the evaporation of hydrated water and conversion of hydroxides into metal oxides. In DTA curve, two sharp peaks appeared at 50 °C and at 248 °C, indicating the exothermic nature of the reaction. Therefore, the weight loss at these temperatures is about 0.148%°C and 2.63%/°C, respectively. The small peak in DTA curve of CFO ferrite noted at a temperature of 50 °C corresponds to the water removal from the sample while the intense sharp exothermic peak observed at 248 °C shows the abrupt decomposition of material to their corresponding oxides. Above 800 °C, no significant weight loss occurs which confirmed the complete phase formation of the prepared ferrite sample. Hence the estimated annealing temperature of the sample under investigation ($CoFe_2O_4$) was taken as 800 °C.

XRD analysis

The XRD graphs of the synthesized $CoEu_xFe_{2-x}O_4$ (x = 0.00–0.12) nanoparticles are given in Fig. 2. The diffraction peaks associated with the Bragg's reflections from (1 1 1), (2 2 0), (3 1 1), (4 0 0), (2 2 2), (4 0 0), (4 2 2), (5 1 1), (4 4 0) and (5 3 3) planes correspond to the typical crystal structure of CFO (JCPDS card # 022-1086) which has spinel face center cubic type belonging to space group of Fd3m. As Eu^{3+} substitution in pure spinel lattice increases, the divergence from single cubic phase becomes clearer with the appearance of secondary phase peaks with insignificant amount of ortho ($EuFeO_3$) and hematite (Fe_2O_3) phases. The development of secondary phases during sintering procedure is governed by

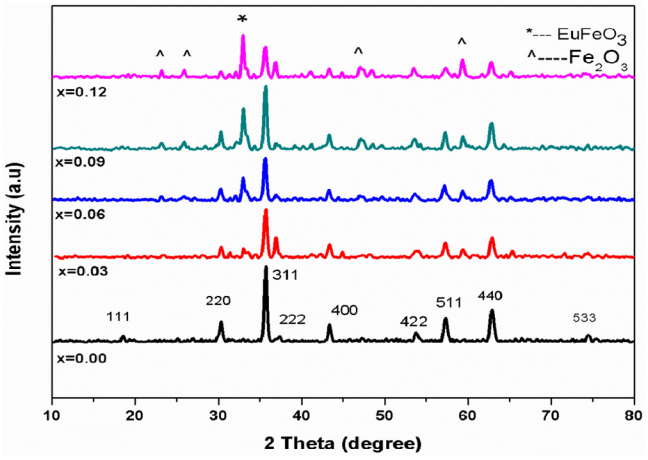

Fig. 2. XRD patterns of $CoEu_xFe_{2-x}O_4$ (x = 0.00–0.12) nanoparticles.

the amount and type of the dopant (Eu^{3+}) used. Therefore, the addition of small amount of Eu^{3+} ions in cobalt ferrite lattice can influence not only the composition of phase but also the size of the spinel matrix. This is possibly due to the presence of hematite and orthoferrite phases [21–24]. It has also been reported earlier that phase formation is significantly affected by the amount of RE elements, in substituted samples of CFO [25]. The main factor for the ortho phase formation in the Eu^{3+} doped CFO samples is ionic radii and electronic configuration of the Eu^{3+} rare earth element. The Eu^{3+} ion with the larger radius of about (1.07 Å) show preference to occupy the octahedral (12k, 4f2, 2a,) sites of Fe^{3+} whose ionic radii is 0.67 Å. Consequently, when the Eu^{3+} ions substitution is high, this directs to the creation of secondary phases as impurity on the grain boundaries due to the diffusion of RE-Eu^{3+} ions. Kamala Bharathi et al. [26] also found a small distortion in the lattice upon the incorporation of Ho for Fe in the B-site and

Table 1
Crystallite size (D), Lattice parameter (a), Cell volume (V_{cell}), X-ray density (Dx), bulk density (Db), porosity and strain of $CoEu_xFe_{2-x}O_4$ (x = 0.00–0.12) nano-ferrites.

Composition	D (nm)	a (Å)	V_{cell} (Å^3)	Dx (g/cm^3)	Db (g/cm^3)	Porosity	Strain
$CoFe_2O_4$	21	8.3646	585.24	5.33	2.72	0.49	0.0048
$CoEu_{0.03}Fe_{1.97}O_4$	19	8.3664	585.62	5.39	2.93	0.46	0.0050
$CoEu_{0.06}Fe_{1.94}O_4$	20	8.3803	588.54	5.43	2.99	0.45	0.0066
$CoEu_{0.09}Fe_{1.91}O_4$	21	8.369	586.17	5.52	3.12	0.43	0.0053
$CoEu_{0.12}Fe_{1.88}O_4$	18	8.3636	585.03	5.59	3.43	0.39	0.0046

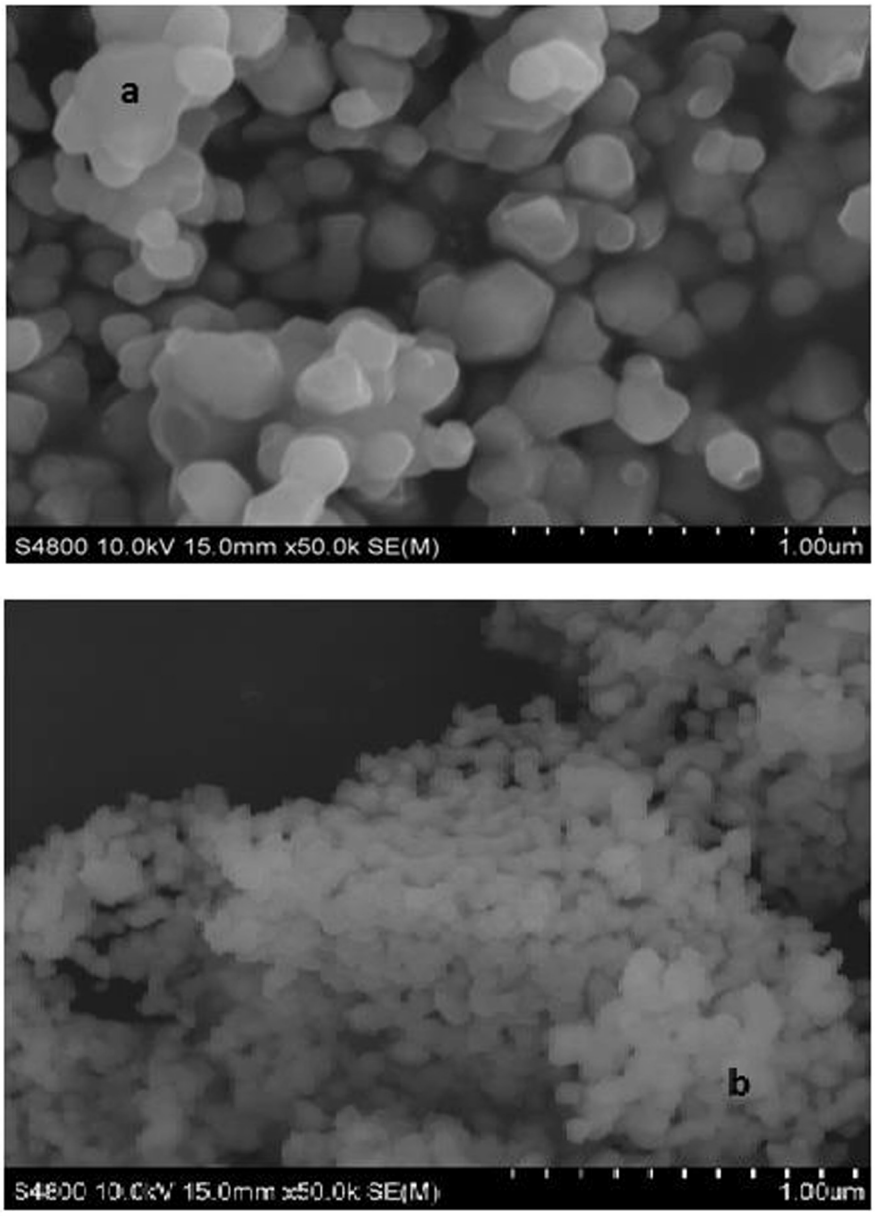

Fig. 3. SEM micrographs of $CoEu_xFe_{2-x}O_4$ ferrites with composition of (a) x = 0 (b) x = 0.12.

may associate this fact to the variations in the O–Co and O–Fe bond lengths in the B-site. The lattice parameter 'a' was determined using the Nelson-Riley function [27];

$$F(\theta) = 1/2[\mathrm{Cos}^2\theta/\mathrm{Sin}\theta + \mathrm{Cos}^2\theta/\theta] \quad (1)$$

It can be seen from Table 1 that lattice constant 'a' increased from 8.365 to 8.380 Å with an increase in Eu^{3+} substitution up to x = 0.06 and decreased thereafter. The increase in 'a' is attributed to substitution of small Fe^{3+} ions by larger Eu^{3+} ions while decrease in 'a' is associated with secondary phases formation. The average value of crystallite size (D) of all samples is estimated from the most intense peak (3 1 1) of XRD patterns. The value of 'D' is calculated using the Scherrer's formula [27];

$$D = k\lambda/\beta\cos\theta \quad (2)$$

where 'D' is the average crystallite size in nm, 'k' is the shape factor with value 0.94, β is FWHM, λ is the wavelength of X-rays used and θ is the Bragg's diffraction angle. Table 1 show that the average crystallite size ranges from 21-18 nm. The variation of densities and lattice strain are also given in Table 1.

SEM

SEM micrographs were taken to examine the grain structure of the nanoparticles and support in understanding the morphology. Fig. 3 depicts the SEM images of the pure cobalt ferrite $CoFe_2O_4$ and Eu^{3+} doped cobalt ferrite. In the present study, it is expected for Eu^{3+} substituted cobalt ferrite that the average grain size decreases with increase in Eu^{3+} substitution. When ferric Fe^{3+} ions in lattice are replaced with by Eu^{3+} ions, the lattice parameter (a) is found to change. This lattice parameter variation will lead to the lattice strains, which create the internal stress. As a result of internal stress, the growth of grains hinders and hence the grain sizes of the Eu^{3+} substituted samples. The existence of Eu^{3+} ions at the boundaries of grains will exert pressure on the grains which also hinder the grains growth.

Energy Dispersive X-ray

Energy Dispersive X-ray (EDX) spectra of Eu doped CFO nanoparticles is shown in Fig. 4. The results confirmed the existence of the constitutive elements Fe, Co and O along with the

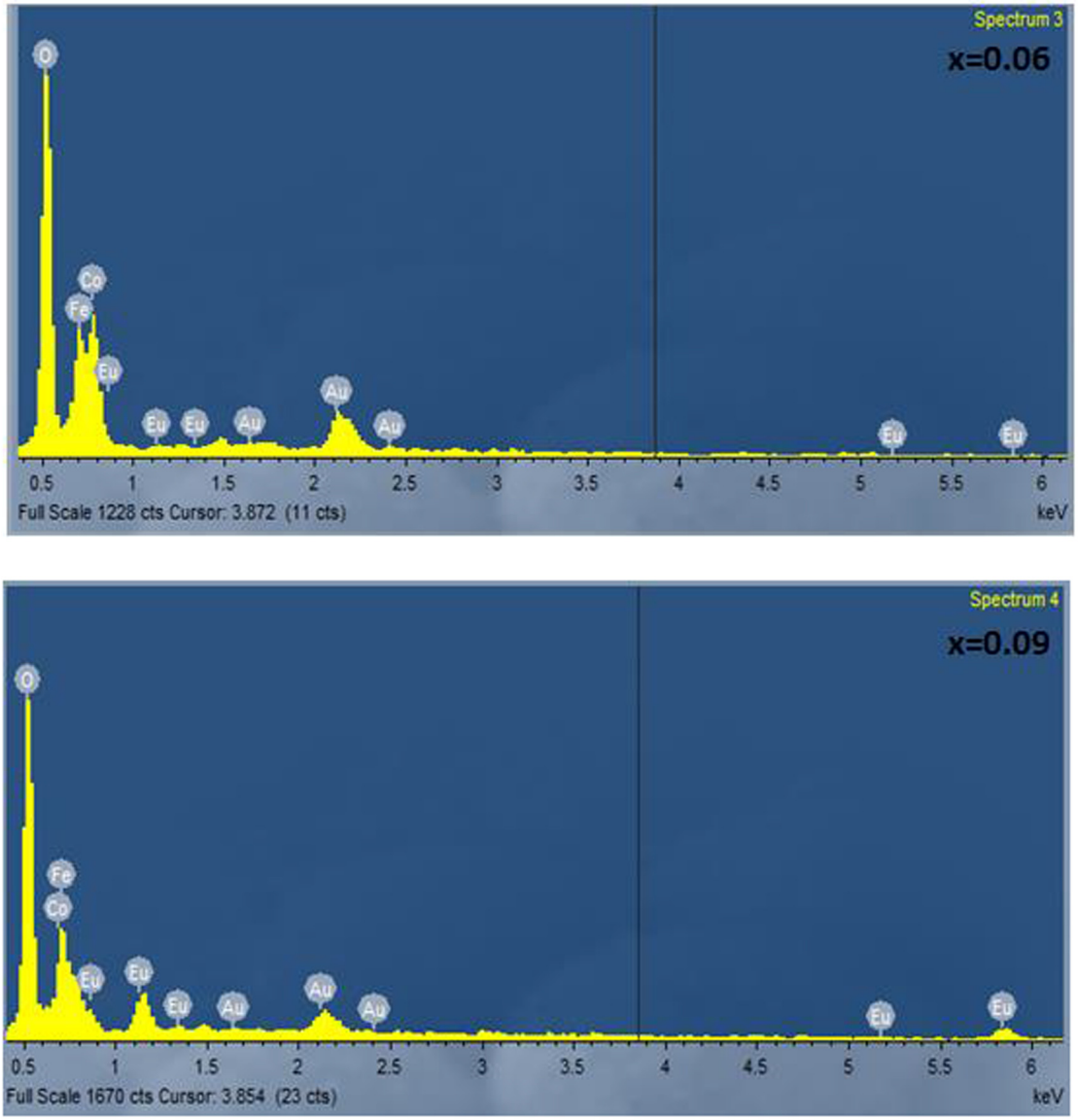

Fig. 4. EDX spectra of $CoEu_xFe_{2-x}O_4$ ferrites with composition of (a) x = 0.06 (b) x = 0.09.

presence of europium content. The EDX spectra illustrate that Eu peaks intensities increase with an increase in europium content. Based on the limits of EDX analysis accuracy, no new chemical elements are identified except Co, Fe, Eu, and O. These results proved that the prepared nanocrystals of ferrites are free of impurities.

Magnetic properties

Magnetic behavior of Eu^{3+} substituted cobalt ferrite nanoparticles was investigated at room temperature with a peak field of ±3 T and the recorded hysteresis loops are shown in Fig. 5. In order to tailor the magnetic properties of the $CoFe_2O_4$ ferrite, ferric ions (Fe^{3+}) are partially substituted by tetravalent nonmagnetic rare earth ions element Eu^{3+}, trying to occupy the octahedral sites and, consequently, the net magnetization decrease. It is noted from Fig. 5 that net magnetization decreases with an increase in Eu^{3+} substitution because of smaller magnetic moment of Eu (3.5 lB) than Fe (5 lB). The magnetic moment of the rare earth ions is generally originated from the localized 4 f-electrons [21]. In spinel ferrites, the saturation magnetization is dominated by the superexchange interactions between the cations of tetrahedral (A) and octahedral (B) sites. According to Neel's model of ferrimagnetism [28], the A-B exchange interactions predominate the intra-sublattice A-A and B-B interactions. As the moments of two sublattices are oppositely directed, the net magnetic moment comes from the difference of the magnetic moments of the A and B sublattices. In terms of magnetizations, relation is $M = M_B\text{-}M_A$, where M_B and M_A are the magnetizations of B and A sub-lattices. According to the distribution of cations, Co^{2+} (3 μB) ions generally contribute to the magnetization of B-site sublattice, Eu^{3+} (3.5 lB) ions participate only to the B-site sublattice magnetization, whereas Fe^{3+} (5 μB) ions make contribution equally to magnetizations of A and B site sublattices. The preferential tenancy of Eu^{3+} ions towards the octahedral sites in the CFO spinel lattice will result in minimizing the number of Fe^{3+} ions at these sites and consequently the net magnetic moment will decrease. The decrease in net magnetization with increasing the Eu^{3+} concentration means that the Fe_A^{3+}–O^{2-}–Eu_B^{3+} superexchange interactions are weaker than the Fe_A^{3+}–O^{2-}–Fe_B^{3+} interactions [29]. The remanence Mr. also increases with increasing the Eu doping. The variation of saturation magnetization and remanence with Eu^{3+} content is shown in Table 2. The anisotropy constant K is calculated using the following relation;

$$K = H_c x M_s/2 \quad (3)$$

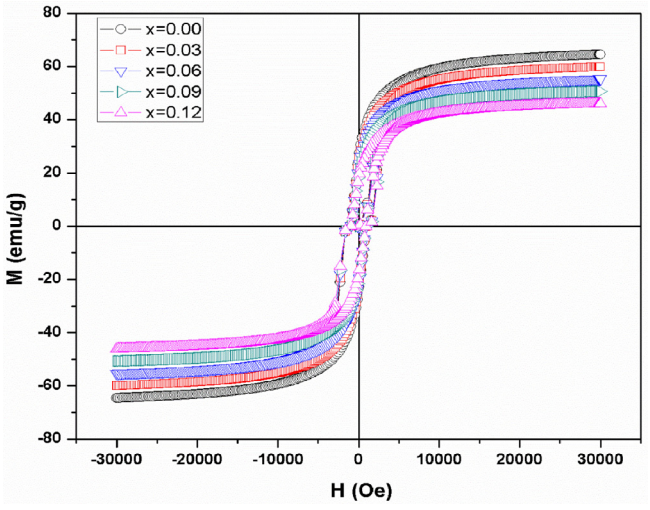

Fig. 5. M–H loops of $CoEu_xFe_{2-x}O_4$ ferrites measured at room temperature.

Table 2
Saturation magnetization (Ms), Coercivity (Hc), anisotropy constant (K) and remanence (Mr) of $CoEu_xFe_{2-x}O_4$ (x = 0.00–0.12) nano-ferrites.

Composition	Ms (emu/g)	Hc (Oe)	Mr (emu/g)	K (erg/cm^3)
$CoFe_2O_4$	65	944	25	30680
$CoEu_{0.03}Fe_{1.97}O_4$	60	937	23.5	28110
$CoEu_{0.06}Fe_{1.94}O_4$	55	959	21.6	26373
$CoEu_{0.09}Fe_{1.91}O_4$	51	954	20	24327
$CoEu_{0.12}Fe_{1.88}O_4$	46	966	18.3	22218

Anisotropy constant K is decreased with increasing the content of Eu and measured values are listed in Table 2 [30]. The reduction in K values indicates the existence of weak grain to grain interactions in these materials. The coercivity Hc increases with Eu^{3+} concentration that may be due to the enhance magneto crystalline anisotropy with anisotropic ferrous Fe^{2+} ions positioned at tetrahedral sites and this occurs due to elevated sintering temperature [31]. The values of coercivity range from 944 Oe to 966 Oe and given in Table 2. Furthermore coercivity considers as microstructure property and depends upon many factors such as surface effect, defects, strains, non-magnetic atoms and strains in the material [32]. The variation of coercive force of the system shows a usual size dependent behavior which can be credited to the combination of surface effect and its surface anisotropy [33]. Moreover, the strong spin orbit coupling of RE Eu^{3+} ions may contribute to the anisotropy while they are positioned at the B-sites of lattice.

Conclusion

The induced effect of Eu-substitution on the thermal behavior, crystal structure, surface morphology and magnetic properties of $CoFe_2O_4$ is significant. TGA studies help out to examine the annealing temperature required for structure formation. Some traces of ortho and hematite phases occur along with primary cubic spinel structure for Eu-content, $x \geq 0.03$. Micro structural features revealed the formation of nanocrystalline grain with spherical morphology. No impurity elements other than constituent atoms are detected in EDX spectra. Magnetic behavior is observed to be strongly dependent on Eu addition and the variation in anisotropy constant is in accordance with the change in coercivity.

Appendix A. Supplementary data

Supplementary data associated with this article can be found, in the online version, at http://dx.doi.org/10.1016/j.rinp.2017.08.035.

References

[1] Andreu I, Natividad E, Ravagli C, Castro M, Baldi G. Heating ability of cobalt ferrite nanoparticles showing dynamic and interaction effects. RSC Adv 2014;4:28968–77.
[2] Mohaideen KK, Joy PA. Enhancement in the magnetostriction of sintered cobalt ferrite by making self-composites from nanocrystalline and bulk powders. ACS Appl Mater Interfaces 2012;4:6421–5.
[3] Rafferty A, Prescott T, Brabazon D. Sintering behaviour of cobalt ferrite ceramic. Ceram Int 2008;34:15–21.
[4] Amiri S, Shokrollahi H. The role of cobalt ferrite magnetic nanoparticles in medical science. Mater Sci Eng C 2013;33:1–8.
[5] Gunjakar J, More A, Shinde V, Lokhande C. Synthesis of nanocrystalline nickel ferrite ($NiFe_2O_4$) thin films using low temperature modified chemical method. J Alloys Compd 2008;465:468–73.
[6] Kolekar Y, Sanchez L, Ramana C. Dielectric relaxations and alternating current conductivity in manganese substituted cobalt ferrite. J Appl Phys 2014;115:144106.
[7] Ramana C, Kolekar Y, Kamala Bharathi K, Sinha B, Ghosh K. Correlation between structural, magnetic, and dielectric properties of manganese substituted cobalt ferrite. J Appl Phys 2013;114:183907.
[8] Kakade SG, Ma Y-R, Devan RS, Kolekar YD, Ramana CV. Dielectric, complex impedance, and electrical transport properties of erbium (Er^{3+}) ion-substituted

nanocrystalline, cobalt-rich ferrite ($Co_{1.1}Fe_{1.9-x}Er_xO_4$). J Phys Chem C 2016;120:5682–93.
[9] Sajjia M, Oubaha M, Hasanuzzaman M, Olabi A. Developments of cobalt ferrite nanoparticles prepared by the sol–gel process. Ceram Int 2014;40:1147–54.
[10] Dascalu G, Popescu T, Feder M, Caltun O. Structural, electric and magnetic properties of $CoFe_{1.8}RE_{0.2}O_4$ (RE = Dy, Gd, La) bulk materials. J Magn Magn Mater 2013;333:69–74.
[11] Mohammadifar Y, Shokrollahi H, Karimi Z, Karimi L. The synthesis of $Co_{1-x}Dy_xFe_{x-2}O_4$ nanoparticles and thin films as well as investigating their magnetic and magneto-optical properties. J Magn Magn Mater 2014;366:44–9.
[12] Zhou B, Zhang Y, Liao C, Yan C, Chen L, Wang S. Enhanced magneto-optical Kerr effects in nanocrystalline Sc-doped $CoFe_2O_4$ thin films. Solid state Commun 2003;126:593–6.
[13] Amiri S, Shokrollahi H. Magnetic and structural properties of RE doped Co-ferrite (REåNd, Eu, and Gd) nano-particles synthesized by co-precipitation. J Magn Magn Mater 2013;345:18–23.
[14] Murugesan C, Chandrasekaran G. Impact of Gd^{3+} substitution on the structural, magnetic and electrical properties of cobalt ferrite nanoparticles. RSC Adv 2015;5:73714–25.
[15] Kadam A, Shinde S, Yadav S, Patil P, Rajpure K. Structural, morphological, electrical and magnetic properties of Dy doped Ni–Co substitutional spinel ferrite. J Magn Magn Mater 2013;329:59–64.
[16] Mahalakshmi S, SrinivasaManja K, Nithiyanantham S. Electrical properties of nanophase ferrites doped with rare earth ions. J Superconduct Novel Magn 2014;27:2083–8.
[17] Kakade S, Kambale R, Kolekar Y, Ramana C. Dielectric, electrical transport and magnetic properties of Er^{3+} substituted nanocrystalline cobalt ferrite. J Phys Chem Solids 2016;98:20–7.
[18] Prathapani S, Vinitha M, Jayaraman TV, Das D. Effect of Er doping on the structural and magnetic properties of cobalt-ferrite. J Appl Phys 2014;115:17A502.
[19] Karimi Z, Mohammadifar Y, Shokrollahi H, Asl SK, Yousefi G, Karimi L. Magnetic and structural properties of nano sized Dy-doped cobalt ferrite synthesized by co-precipitation. J Magn Magn Mater 2014;361:150–6.
[20] Bünzli J-C, Choppin GR. Lanthanide probes in life. Chem Earth Sci 1989.
[21] Shirsath SE, Mane ML, Yasukawa Y, Liu X, Morisako A. Self-ignited high temperature synthesis and enhanced super-exchange interactions of Ho^{3+}–Mn^{2+}–Fe^{3+}–O^{2-} ferromagnetic nanoparticles. Phys Chem Chem Phys 2014;16:2347–57.
[22] Bhowmik R, Ranganathan R. Magnetic properties in rare-earth substituted spinel $Co_{0.2}Zn_{0.8}Fe_{2-x}RE_xO_4$ (RE = Dy, Ho and Er, x = 0.05). J Alloys Compd 2001;326:128–31.
[23] Naseri MG, Saion EB, Ahangar HA, Shaari AH, Hashim M. Simple synthesis and characterization of cobalt ferrite nanoparticles by a thermal treatment method. J Nanomater 2010;2010:75.
[24] Naseri MG, Saion EB, Ahangar HA, Hashim M, Shaari AH. Simple preparation and characterization of nickel ferrite nanocrystals by a thermal treatment method. Powder Technol 2011;212:80–8.
[25] Ateia E, Ahmed M, El-Aziz A. Effect of rare earth radius and concentration on the structural and transport properties of doped Mn–Zn ferrite. J Magn Magn Mater 2007;311:545–54.
[26] Bharathi KK, Markandeyulu G, Ramana C. Structural, magnetic, electrical, and magnetoelectric properties of Sm-and Ho-substituted nickel ferrites. J Phys Chem C 2010;115:554–60.
[27] Cullity B. Element of X-ray Diffraction. MA Google Scholar: Addison-Wesley Reading; 1978.
[28] Standley KJ. Oxide Magnetic Materials. Oxford University Press; 1972.
[29] Ounnunkad S. Improving magnetic properties of barium hexaferrites by La or Pr substitution. Solid State Commun 2006;138:472–5.
[30] Ali I, Islam M, Ishaque M, Khan HM, Ashiq MN, Rana M. Structural and magnetic properties of holmium substituted cobalt ferrites synthesized by chemical co-precipitation method. J Magn Magn Mater 2012;324:3773–7.
[31] Aen F, Niazi SB, Islam M, Ahmad M, Rana M. Effect of holmium on the magnetic and electrical properties of barium based W-type hexagonal ferrites. Ceram Int 2011;37:1725–9.
[32] Roy P, Nayak BB, Bera J. Study on electro-magnetic properties of La substituted Ni–Cu–Zn ferrite synthesized by auto-combustion method. J Magn Magn Mater 2008;320:1128–32.
[33] Shirsath SE, Kadam R, Gaikwad AS, Ghasemi A, Morisako A. Effect of sintering temperature and the particle size on the structural and magnetic properties of nanocrystalline $Li_{0.5}Fe_{2.5}O_4$. J Magn Magn Mater 2011;323:3104–8.